

© 2021. X.J. Zhang, H.M. An.

This is an open-access article distributed under the terms of the Creative Commons Attribution-NonCommercial-NoDerivatives License (CC BY-NC-ND 4.0, <https://creativecommons.org/licenses/by-nc-nd/4.0/>), which permits use, distribution, and reproduction in any medium, provided that the Article is properly cited, the use is non-commercial, and no modifications or adaptations are made.



ANALYSIS OF POSITIVE ELEVATION EFFECT AND PREDICTION OF VIBRATION VELOCITY OF BENCH BLASTING VIBRATION

X.J. ZHANG¹, H.M. AN²

Accurate prediction of blasting vibration should be achieved in mine blasting production practice. It is also a critical problem in the field of blasting vibration control technology research. In this research paper, on the basis of the previous research results and taking account into the reflection principle of elastic wave at the free interface, the authors propose the blasting seismic wave propagation model. In addition, the blasting positive elevation effect are theoretically explained in detail, and the vibration velocity prediction formula of the positive elevation effect is derived. Finally, the positive elevation effect mechanism and the step (positive) formula are calibrated based on the on-site monitoring data of blasting vibration of Qipanjiang Jinou coal mine. In brief, a theoretical basis is laid by this paper for similar blasting projects.

Keywords: Blasting Vibration, positive elevation effect, step (positive) formula

¹ PhD., Eng., School of Civil and Resource Engineering, University of Science and Technology Beijing, Beijing 100083, China.

² Lecturer, PhD., Eng., Kunming University of Science and Technology, Faculty of Public Security and Emergency Management, 650093, Kunming, China. H.M. An (Huaming An) is the corresponding author.

* Corresponding author (H.M.An): email : Huaming.an@yahoo.com

1. INTRODUCTION

On the whole, large-scale open pit mines have a large blasting scale and frequent blasting operations. Accordingly, the vibration attributed to blasting is a vital factor affecting the safety of blasting and the stability of slope rock mass. For this reason, accurate prediction of blasting vibration should be achieved in mine blasting production practice. It is also a critical problem in the study of blasting vibration control technology.

As the study on blasting vibration in open pit mine has been deepened, people gradually realize the elevation effect of high-difference terrain blasting vibration [1-5]. Nachiket V. Bhagade et al. [6] used seismic tomography using 24-channels to characterize the rockmass, and used two Triaxial Borehole Feophones to record ground vibrations. High values of vertical peak particle velocity (PPV) was recorded indicating that long column charges and large diameter holes are responsible for massive cratering and resultant seismic impacts. Tan Wenhui et al. [7], by analyzing the experimental data under the blast conditions with different height differences, drew the conclusion that the values of the parameters k and a of the Sadowski formula are associated with the lithology of the propagation medium. Navarro Torres V.F. et al. [8] collected 178 levels of blasting-induced vibrations data in a large open-pit iron ore mine, and then used multiple regression techniques to process data and obtain the blasting vibration attenuation law. Then, according to international admissibility standards and the minimum distance between the mine and community, the maximum explosive charge per delay could be established. Chen Ming et al. [9] analyzed the blasting vibration velocity under different height difference conditions using numerical simulation method, and concluded that the vibration velocity of the slope bench rock mass has an amplification effect, when the slope shape varies suddenly and the slope increases. Havenith et al. [10] studied the blasting vibration velocity through finite element software and concluded that local factors affect the amplification effect of blasting vibration wave. Hoang Nguyen et al. [11] used boosted generalized additive models (BGAMs), support vector machine (SVM) and artificial neural network (ANN) to predict blast-induced peak particle velocity. Results revealed that the proposed BGAM performed better than the other models, and the elevation difference between the blasting site and monitoring point is one of the dominant parameters governing the PPV predictive models. Hamid Reza Mohammadi Azizabadi et al. [12] used coupling of two methods, waveform superposition and numerical, to model blast vibration effect on slope stability in the Gol-E-Gohar iron mine. The final conclusion was that the maximum displacement at the crest of the nearest bench was 26mm, which is acceptable in regard to open pit

slope stability. Hu Xuelong et al.[13] analyzed the effect of terrain on the propagation path of blasting seismic waves. They also proposed two concepts (equivalent path and equivalent distance). Guo Xuebin et al. [14], based on the field test results of blasting vibration, primarily analyzed and discussed the slope effect. Zhou Tongling et al.[15], through the experimental observation of the seismic effect of the positive and negative elevation terrain blasting, drew the conclusions that the positive elevation causes the seismic effect to increase and the negative height difference causes the seismic effect to decrease. Feng Zhiren et al.[16] borrowed *FLAC^{3D}* software to build a numerical model for dynamic analysis of bedding rock slopes with weak interlayers. Moreover, they analyzed the surface amplification effect under the effect of ground motion velocity peak, frequency, duration as well as initial direction.

However, above research primarily focuses on on-site monitoring and numerical simulation[17-19], and there has been no scientific and unified understanding of the mechanism of generating elevation effects. Thus, based on previous research results, the positive elevation effect of blasting vibration is theoretically explained in this paper by building the blasting seismic wave propagation model in accordance with the reflection principle of elastic wave at the free interface. Lastly, the positive elevation effect mechanism and the step (positive) formula are verified based on the on-site monitoring data of blasting vibration of Qipanjing Jinou Coal Mine. This paper lays a theoretical basis for blasting design and safety monitoring of high slope engineering.

2. MECHANISM ANALYSIS OF POSITIVE ELEVATION EFFECT OF BLASTING VIBRATION

It is assumed that the underground rock formation is isotropic and the explosion source is spherically symmetric. Blasting seismic waves propagate in the formation in the form of spherical waves. At the same time, the ground is assumed to be a free surface. After the seismic waves reach the ground, they are reflected and superimposed on the ground. By comparing the reflection of the flat ground model and the step model on the free surface, the positive elevation effect of blasting vibration is explained. The main theory used here is the theory of elastic spherical wave propagation in uniform and isotropic media. There is also the reflection theory of elastic waves on free surfaces. In the process of elastic wave reflection analysis on free surface, a representative longitudinal (p) wave is analyzed.

2.1 PROPAGATION OF BLASTING VIBRATION ELASTIC WAVE

Given that the seismic wave caused by blasting is an elastic wave propagating in a subterranean formation, the source of the explosion is assumed to be spherically symmetric. Subsequently, after the seismic wave propagates to the rock mass and does not reach the ground, it can be considered a divergent spherical wave [20]. If there are both primary (P) wave components and secondary (S) wave components in the spherical wave, then set u_p 、 u_s denote their displacement field respectively, u is the total displacement field. And φ and ψ represent the scalar and vector potential of the displacement field[21], and:

$$u = u_p + u_s = \nabla\varphi + \nabla \times \psi \quad (1)$$

Taking P wave as an example, and:

$$\varphi = \frac{A}{r} \exp[i(kr - wt)], r > 0 \quad (2)$$

The displacement vector field is:

$$u_p = \nabla\varphi = \frac{\partial\varphi}{\partial r} e_r = A\left(\frac{ik}{r} - \frac{1}{r^2}\right) \exp[i(kr - wt)] e_r \quad (3)$$

Where A denotes the amplitude of ψ at the source, equal to a constant, w is the circular frequency of the wave, and $k = w/c = 2\pi/\lambda$ is the number of circular waves. r is the distance from the observation point to the source, when $r \gg \lambda$, there is $1/\lambda \geq 1/r$, Comparing the two brackets in Eq. (3), we can omit $1/r^2$, and then Eq. (3) becomes:

$$u_p = \frac{ikA}{r} \exp[i(kr - wt)] e_r \quad (4)$$

The simple harmonic of the spherical displacement is expressed in Eq. (4), suggesting that the amplitude of the displacement at a distance away from the source is inversely proportional to the distance from the source.

The magnitude of the displacement of the wave calculated by Eq. (4) is expressed as:

$$u_p = \frac{A}{r} e^{i(kr - wt)} \quad (5)$$

The above equation is adopted to derive the time t . Then, the vibration velocity of the particle at the observation point is expressed as:

$$C_p = -w \frac{A}{r} e^{i(kr - wt)} \quad (6)$$

2.2 REFLECTION OF ELASTIC WAVES ON FREE SURFACES

A free surface is a special interface setting the boundary between the medium and the vacuum, i.e. no medium exists on one side of the interface. In practice, we are treating the surface of the earth as a free surface[22]. Fig. 1 suggests that the x-y plane is taken as a free surface. A P wave is placed from the lower medium onto the free surface. Since there is no medium on the surface, when the wave encounters the boundary of the medium, it can only be transferred back to the original medium without passing through it, i.e. only the reflected wave exists, and there is no transmitted wave. When the P wave is incident on the free surface, it will cause not only displacement along the normal direction of the surface, but also displacement along the tangential direction. Accordingly, the reflected wave contains both P wave and SV wave components. However, depending on the symmetry of the problem and the independence of the P wave, SV wave and SH wave, the reflected wave does not contain the SH wave component.

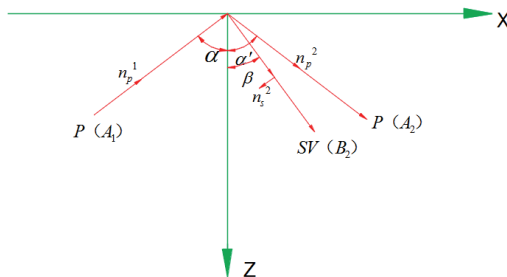


Figure 1 P wave incidence

The displacement vectors of the incident P wave, the reflected P wave, and the reflected SV wave are defined as follows.[22]

$$\left. \begin{aligned}
 \vec{s}_P^1 &= j \frac{w}{V_p} A_1 e^{j(k_x x + k_z z - wt)} \vec{n}_p^1 \\
 \vec{s}_P^2 &= j \frac{w}{V_p} A_2 e^{j(k_x' x + k_z' z - wt)} \vec{n}_p^2 \\
 \vec{s}_S^2 &= j \frac{w}{V_s} B_2 e^{j(k_x'' x + k_z'' z - wt)} \vec{n}_s^2
 \end{aligned} \right\} \quad (7)$$

Where w denotes the circular frequency of the wave; V_p and V_s are the speeds of the P and S waves, respectively; A_1 、 A_2 、 B_2 are the amplitudes of each wave function; \vec{n}_p^1 、 \vec{n}_p^2 、 \vec{n}_s^2 is the unit vector.

According to the propagation law of harmonics at the interface, at the free surface $z=0$, the magnitude of the displacement of each wave is defined as follows.

$$\left. \begin{aligned} S_p^1 &= \frac{w}{V_p} A_1 e^{j(k_x x - wt)} \\ S_p^2 &= \frac{w}{V_p} A_2 e^{j(k_x x - wt)} \\ S_s^2 &= \frac{w}{V_s} B_2 e^{j(k_x x - wt)} \end{aligned} \right\} \quad (8)$$

The above displacement expression is adopted to derive the time t , and the velocity of the mass at the observation point caused by the harmonic is calculated as:

$$\left. \begin{aligned} C_p^1 &= -\frac{w^2}{V_p} A_1 e^{j(k_x x - wt)} \\ C_p^2 &= -\frac{w^2}{V_p} A_2 e^{j(k_x x - wt)} \\ C_s^2 &= -\frac{w^2}{V_s} B_2 e^{j(k_x x - wt)} \end{aligned} \right\} \quad (9)$$

In line with the geometric relationship, when the reflected P wave and the reflected SV wave are superimposed, the particle velocity at the free surface can be respectively expressed in the x direction and the z direction as follows.

$$\left. \begin{aligned} C_x &= C_p^2 \sin a - C_s^2 \cos \beta \\ C_z &= C_p^2 \cos a + C_s^2 \sin \beta \end{aligned} \right\} \quad (10)$$

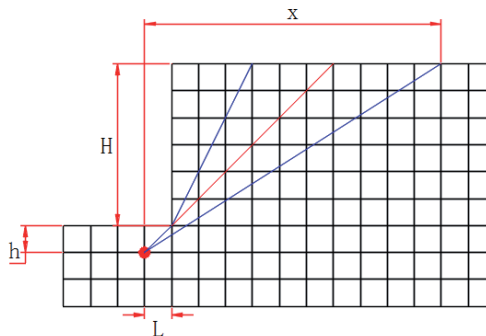
2.3 ANALYSIS OF THE MECHANISM OF POSITIVE ELEVATION EFFECT OF STEP BLASTING VIBRATION

To study the mechanism of the positive elevation effect of the step blasting vibration, a geometric model is built, as shown in Fig. 2. Assume that the step model is a high-steep shape, the observation

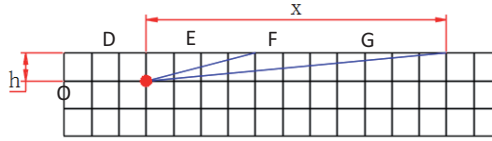
point has a certain distance from the source, and the depth of the explosive is shallow. In the step model, the distance between the blasthole and the edge of the step is almost equal to the depth of the explosive. Set the depth of the medicine package as h , the height of the step as H , the distance between the medicine package and the edge of the step as l , and the horizontal distance of the observation point from the medicine package as x . Following the Huygens-Fresnel principle, each point on the wavefront (wavefront) can be considered the wave source of the transmitted wavelet in the propagation process. At any subsequent time, the envelope surface of these wavelets will become a new wavefront. The new wavefront is superimposed by the interference of each wavelet on the wavefront. In the meantime, according to the Fermat principle, the waves always propagate along the path with the smallest propagation time in the medium. These paths are rays, and the rays are straight lines in a uniform medium. Subsequently, from the source to the observation point E, the path of the seismic wave propagation in the step model is represented as $O-D-E$, and the path propagated in the flat model is expressed as $O-E$, O is the center of the explosion source, as shown in Fig. 2.

According to the Eq. (10), in the step model, the diagram a in Fig. 2, the elastic waves are superimposed on each other at the free surface E, and they can be respectively expressed in the 1 direction and the 1 direction as:

$$\left. \begin{aligned} C_{x1} &= C_p^{2'} \sin a_1 - C_s^{2'} \cos \beta_1 \\ C_{z1} &= C_p^{2'} \cos a_1 + C_s^{2'} \sin \beta_1 \end{aligned} \right\} \quad (11)$$



(a)step model



(b) Flat model

Figure 2 Step model and flat model

In the flat model, the diagram b in Fig. 2, the elastic waves are superimposed on each other at the free surface E, which are respectively expressed in the X and Z directions as follows.

$$\left. \begin{aligned} C_{x2} &= C_p^{2''} \sin \alpha_2 - C_s^{2''} \cos \beta_2 \\ C_{z2} &= C_p^{2''} \cos \alpha_2 + C_s^{2''} \sin \beta_2 \end{aligned} \right\} \quad (12)$$

Where α_1 , β_1 denote the angle of incidence and the angle of reflection of the wave at a point in the step model, respectively. α_2 , β_2 are the incident angle and reflection angle of the wave at a certain point in the flat model.

In the step model, compared with the flat model, at the observation point where the horizontal distance from the center of the explosion source is equal. The vibration speed amplification factor can be respectively expressed in the X direction and the Z direction as:

$$R_{cxT} = \frac{C_{x1}}{C_{x2}} \quad (13)$$

$$R_{czT} = \frac{C_{z1}}{C_{z2}} \quad (14)$$

Substituting the Eq. (11) and (12) into the above formula, and further simplifying the formula according to the Eq. (9), it yields:

$$\begin{aligned} R_{cxT} &= \frac{A_2' \sin \alpha_1 - \frac{V_p}{V_s} B_2' \cos \beta_1}{A_2'' \sin \alpha_2 - \frac{V_p}{V_s} B_2'' \cos \beta_2} \\ &= \frac{A_1'}{A_1''} \frac{A_2' \sin \alpha_1 - \frac{V_p}{V_s} B_2' \cos \beta_1}{A_2'' \sin \alpha_2 - \frac{V_p}{V_s} B_2'' \cos \beta_2} \end{aligned} \quad (15)$$

$$\begin{aligned}
 R_{czT} &= \frac{A_2' \cos \alpha_1 + \frac{V_p}{V_s} B_2' \sin \beta_1}{A_2'' \cos \alpha_2 + \frac{V_p}{V_s} B_2'' \sin \beta_2} \\
 &= \frac{\frac{A_2'}{A_1'} \cos \alpha_1 + \frac{V_p}{V_s} \frac{B_2'}{A_1'} \sin \beta_1}{\frac{A_2''}{A_1''} \cos \alpha_2 + \frac{V_p}{V_s} \frac{B_2''}{A_1''} \sin \beta_2}
 \end{aligned} \quad (16)$$

Where $\frac{A_2'}{A_1'}$, $\frac{B_2'}{A_1'}$, $\frac{A_2''}{A_1''}$ and $\frac{B_2''}{A_1''}$ are called reflection coefficients of P and SV waves, respectively [23].

$$\left. \begin{aligned}
 \frac{A_2'}{A_1'} &= \frac{V_s^2 \sin 2\alpha_1 \sin 2\beta_1 - V_p^2 \cos^2 2\beta_1}{V_s^2 \sin 2\alpha_1 \sin 2\beta_1 + V_p^2 \cos^2 2\beta_1} \\
 \frac{B_2'}{A_1'} &= \frac{-2V_s^2 \sin 2\alpha_1 \cos 2\beta_1}{V_s^2 \sin 2\alpha_1 \sin 2\beta_1 + V_p^2 \cos^2 2\beta_1}
 \end{aligned} \right\} \quad (17)$$

$$\left. \begin{aligned}
 \frac{A_2''}{A_1''} &= \frac{V_s^2 \sin 2\alpha_2 \sin 2\beta_2 - V_p^2 \cos^2 2\beta_2}{V_s^2 \sin 2\alpha_2 \sin 2\beta_2 + V_p^2 \cos^2 2\beta_2} \\
 \frac{B_2''}{A_1''} &= \frac{-2V_s^2 \sin 2\alpha_2 \cos 2\beta_2}{V_s^2 \sin 2\alpha_2 \sin 2\beta_2 + V_p^2 \cos^2 2\beta_2}
 \end{aligned} \right\} \quad (18)$$

In the step model, according to Eq. (6), the velocity of the particle at the observation point E (the elastic wave does not reach the critical point of the free surface) is:

$$C_{p1}' = -w \frac{A}{\sqrt{(H-h)^2 + l^2} \times (x-l)} e^{i(kr-wt)} \quad (19)$$

Subsequently the particle vibration velocity amplitude is:

$$A_1' = -w \frac{A}{\sqrt{(H-h)^2 + l^2} \times (x-l)} \quad (20)$$

In the flat model, according to Eq. (6), the velocity of the particle at the observation point E (the elastic wave does not reach the critical point of the free surface) is

$$C_{p1}'' = -w \frac{A}{\sqrt{h^2 + x^2}} e^{i(kr-wt)} \quad (21)$$

Subsequently its particle vibration velocity amplitude is:

$$A_1'' = -w \frac{A}{\sqrt{h^2 + x^2}} \quad (22)$$

Then

$$\frac{A_1'}{A_1''} = \frac{\sqrt{h^2 + x^2}}{\sqrt{(H-h)^2 + l^2} \times (x-l)} \quad (23)$$

The relationship between the velocity ratio of the elastic longitudinal wave and the transverse wave and the Poisson's ratio is expressed as [24]:

$$\frac{V_p}{V_s} = \sqrt{\frac{2(1-\nu)}{1-2\nu}} \quad (24)$$

According to Snell's law, it yields:

$$\frac{V_p}{V_s} = \frac{\sin \alpha}{\sin \beta} \quad (25)$$

3. ESTABLISHMENT OF VIBRATION VELOCITY PREDICTION FORMULA OF POSITIVE STEP BLASTING

3.1 ANALYTIC SIMPLIFICATION OF AMPLIFICATION FACTOR OF POSITIVE ELEVATION EFFECT VIBRATION SPEED

In large-scale deep open pit mines, the general step slope is relatively high and steep. And the observation point has a certain distance from the source. In the meantime, according to the assumptions of the step model and the flat model, the analytic formula of the positive elevation effect is further approximated. The table suggests that Poisson's ratio varies from 0 to 0.5, and the Poisson's ratio of the general rock is around 0.25.

$$\nu = 0.25 \quad (26)$$

(1) Near source area (DF section)

In the step model, the DF segment, the elastic p wave incident angle α_1 is relatively small, between 0 and 45 degrees. In practical engineering applications, the vibration velocity near the step is highlighted. To simplify the calculation, taking a specific point to represent the value of α_1 , taking $\alpha_1 = 20^\circ$. Subsequently, according to Eq. (24), Eq. (25), and Eq. (17) and (18):

$$\left. \begin{aligned} \beta_1 &= 11.39^\circ \\ \frac{A'_2}{A'_1} &= -0.8222 \\ \frac{B'_2}{A'_1} &= -0.4235 \end{aligned} \right\} \quad (27)$$

In the flat model, the DF segment, the near source of the explosion source. The angle α_2 of incidence of the elastic P wave is larger than the step model, which is between 45 and 80° . So to simplify the calculation, take a specific point to represent the value of α_2 , take $\alpha_2 = 60^\circ$ then:

$$\left. \begin{aligned} \beta_2 &= 30^\circ \\ \frac{A''_2}{A''_1} &= -2.9342 \times 10^{-5} \approx 0 \\ \frac{B''_2}{A''_1} &= -0.5775 \end{aligned} \right\} \quad (28)$$

According to the conditions of the initial hypothesis, the step is high and steep, and the observation point has a certain distance from the source. Thus, the depth h of the explosive is relatively small, compared with the distance from the observation point, which is negligible. And the depth of the explosive is approximately equal to the distance from the blasthole to the edge of the step, then:

$$h \approx L \quad (29)$$

Subsequently according to Eq. (23).

$$\begin{aligned} \frac{A'_1}{A''_1} &= \frac{\sqrt{x^2 + h^2}}{\sqrt{h^2 + h^2} \times \sqrt{(x-h)^2 + H^2}} \\ &= \frac{x}{\sqrt{2}h \times \sqrt{x^2 + H^2}} \end{aligned} \quad (30)$$

Substituting Eq. (27), (28), and (30) into Eq. (15) and (16):

$$\left. \begin{aligned} R_{cxt} &= 1.3 \frac{x}{\sqrt{2}h \times \sqrt{x^2 + H^2}} \\ R_{czt} &= 1.8 \frac{x}{\sqrt{2}h \times \sqrt{x^2 + H^2}} \end{aligned} \right\} \quad (31)$$

For a particular project, h is a certain value.

(2) Explosion source far area (FG section)

In the step model, the incident angle α_1 of the elastic P wave ranges from 45 to 90° . As the value of x increases, α_1 will approach 90° . In the flat model, the incident angle α_2 of the elastic P wave ranges from 80 to 90° . As the value of x increases, α_2 will approach 90° . In the meantime, compared with the step model, at the measuring point where the horizontal distance x is equal, $\alpha_1 < \alpha_2$. To simplify the calculation, make $\alpha_1 = 70^\circ$, $\alpha_2 = 85^\circ$, Subsequently, according to Eq. (24), Eq. (25), and Eq. (17), Eq. (18).

$$\left. \begin{aligned} \beta_1 &= 32.86^\circ \\ \frac{A'_2}{A'_1} &= 0.0720 \\ \frac{B'_2}{A'_1} &= -0.4836 \end{aligned} \right\} \quad (32)$$

$$\left. \begin{aligned} \beta_2 &= 35.11^\circ \\ \frac{A''_2}{A''_1} &= -0.3554 \\ \frac{B''_2}{A''_1} &= -0.2318 \end{aligned} \right\} \quad (33)$$

According to the conditions of the initial hypothesis, the steps are steep and the observation point has a certain distance from the source. Accordingly, the depth h of the explosive is relatively small, compared with the distance from the observation point to the source. It is negligible.

$$\frac{A'_1}{A''_1} = \frac{\sqrt{x^2 + h^2}}{\sqrt{x^2 + (h+H)^2}} = \frac{x}{\sqrt{x^2 + (h+H)^2}} \quad (34)$$

Because it is a high steep step, the depth h of the explosive is relatively small, compared with the elevation difference H , so it is neglected. It is further simplified:

$$\frac{A'_1}{A''_1} = \frac{x}{\sqrt{x^2 + H^2}} \quad (35)$$

Substituting Eq. (32), (33), and (35) into Eq. (15) and (16)

$$\left. \begin{aligned} R_{c\alpha T} &= -30.1 \left[\frac{x}{\sqrt{x^2 + H^2}} \right] \\ R_{c\alpha T} &= 1.6 \left[\frac{x}{\sqrt{x^2 + H^2}} \right] \end{aligned} \right\} \quad (36)$$

The Eq. (31) and (36) are unified, and the parameter k_1 is introduced, i.e. the step model positive elevation vibration speed amplification factor R_{cT} can be expressed as:

$$R_{cT} = k_1 \left[\left(\frac{x}{\sqrt{x^2 + H^2}} \right) \right] \quad (37)$$

To reduce the error caused by the approximation in the above process of simplification, the parameter β is introduced, and the Eq. (37) is written as:

$$R_{cT} = k_1 \left[\left(\frac{x}{\sqrt{x^2 + H^2}} \right) \right]^\beta \quad (38)$$

3.2 PREDICTION FORMULA OF POSITIVE ELEVATION EFFECT VIBRATION VELOCITY

Set the vibration speed at the blasting observation point of the positive elevation step model as V_p . Based on the Sadowski formula, the prediction formula for the vibration velocity of observation points widely used in flat terrain is [25]:

$$V = k \left(\frac{Q^{1/3}}{R} \right)^\alpha \quad (39)$$

In the formula: V — Ground particle peak vibration velocity, cm/s;

Q — The number of explosives (the total charge during the explosion, the maximum charge during the delayed blast), Kg;

R — The distance from the observation point (calculation point) to the explosion source, m;

k, α — The coefficient and attenuation coefficient associated with the topography and geological conditions between the blasting point and the calculation point.

Subsequently, the vibration speed V_p of the positive elevation step model blasting observation point is compared with the vibration speed of the flat terrain, and the magnification is expressed as:

$$R_{cT} = \frac{V_p}{V} \quad (40)$$

Then according to Eq. (37)

$$V_p = R_{cT} \cdot V = k_1 k \left(\frac{Q^{1/3}}{R} \right)^\alpha \left(\frac{x}{\sqrt{x^2 + H^2}} \right)^\beta \quad (41)$$

$$K = k_1 k_2 \quad (42)$$

Subsequently Eq. (41) is written as:

$$V_p = K \left(\frac{Q^{1/3}}{R} \right)^\alpha \left(\frac{x}{\sqrt{x^2 + H^2}} \right)^\beta \quad (43)$$

Eq. (43) is the formula for predicting the vibration speed of the elevation model of the step model, step (positive) formula. Since R denotes the explosion source distance, and x is the horizontal distance from the center of the explosion source, the above formula can also be written as:

$$V_p = K \left(\frac{Q^{1/3}}{\sqrt{D^2 + H^2}} \right)^\alpha \left(\frac{D}{\sqrt{D^2 + H^2}} \right)^\beta \quad (44)$$

where V_p — The peak vibration velocity of the ground level of the positive elevation step, cm/s;

Q — The number of explosives (the total charge during the explosion, the maximum charge during the delayed blast), Kg;

D — The horizontal distance from the observation point (calculation point) to the explosion source, m;

D — The vertical distance from the observation point (calculation point) to the explosion source, m;

k, α — The coefficient and attenuation coefficient associated with the topography and geological conditions between the blasting point and the calculation point;

β — Error coefficient;

4. ON-SITE BENCH BLASTING VIBRATION MONITORING

4.1 FIELD MEASUREMENT AND ANALYSIS OF BLASTING VIBRATION

Jinou Coal Mine of Etuoqeqi, Inner Mongolia Autonomous Region (hereinafter referred to as Jinou Coal Mine) is located in Heilonggui Mining Area, Qipanjiang, Etuoqe Banner, Erdos City. The administrative division of Jinou Coal Mine belongs to the Etuoqe Banner Albas Sumu. The mining area is about 1.472km² and the mining elevation is 1270-1040m. The TC-4850 blasting vibrometer produced by Chengdu Zhongke Measurement & Control Co., Ltd. was used in this test. The data obtained from monitoring on October 13 are listed in Table 1.

From the monitoring data of Table 1, the distribution law of the vibration velocity with the horizontal distance of the explosion source can be plotted, as shown in Fig. 3.

Table 1 Measurement point blasting vibration monitoring data

Date	Single dose (kg)	Measuring point number	Distance from the source		Vibration speed (cm/s)
			Level (m)	vertical (m)	
10.13	160	1	142	25	2.128
		2	162	25	1.623
		3	188	35	1.918
		4	227	35	1.183
		5	241	33.8	1.108
		6	252	33.8	0.912
		7	344	118	0.425
		8	354	118	0.337
		9	393	165	0.238

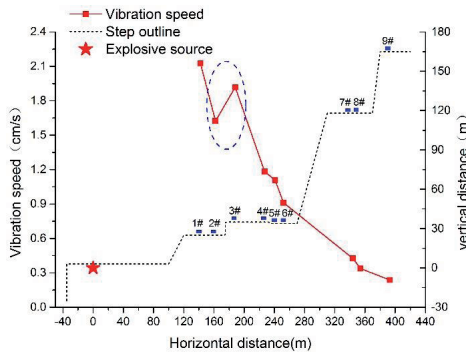


Figure 3. Vibration velocity of measuring point

Fig. 3 suggests that the vibration velocity of the 3# measuring point is enlarged compared with the 2# measuring point. The vibration velocity of the other measuring points decreases gradually, with the rise in the horizontal distance. The vibration velocity curve is steeper near the explosion source, and the vibration velocity curve is gentler in the far zone, which reveals that the vibration velocity decays rapidly near the explosion source, and the attenuation is slow in the far region.

4.2 REGRESSION ANALYSIS OF PREDICTION FORMULA FOR POSITIVE ELEVATION EFFECT

In this section, the methodologies for rock mechanism test under static and dynamic loads are introduced. The uniaxial compressive strength test is employed to model the rock fracture process under static load while the split Hopkinson pressure bar is used to carry out the dynamic rock fracture test.

Some researchers hold that the commonly used Sadowski formula only considers the vibration velocity V with the rise in the explosion source distance R , and it does not consider the effect of elevation on the blasting vibration effect. Thus, some optimized formulas are proposed, e.g., the Sadowski Eq. (space distance formula) :

$$V = K \left(\frac{Q^{1/3}}{\sqrt{D^2 + H^2}} \right)^a \quad (45)$$

Where: D denotes the horizontal distance (m) between the observation point and the source; H is the vertical distance between the observation point and the source.

While some literature [26, 27] considered the elevation effect of blasting vibration wave propagation, the optimized particle vibration velocity formula is proposed :

$$V = K \left(\frac{Q^{1/3}}{D} \right)^a \left(\frac{Q^{1/3}}{H} \right)^\beta \quad (46)$$

Zhu Chuantong et al. [28] considered that the vibration velocity has an amplification effect along the elevation, and accordingly the calculation of the vibration velocity is considered as:

$$V = K \left(\frac{Q^{1/3}}{R} \right)^a \left(\frac{Q^{1/3}}{H} \right)^\beta \quad (47)$$

Where: R denotes the explosion source distance, i.e. the distance between the center of the explosion source and the measuring point (m), which is written as:

$$R = \sqrt{D^2 + H^2} \quad (48)$$

Tang Hai [29] et al. obtained an optimized calculation formula reflecting the elevation amplification effect using the dimensional analysis method:

$$V = K \left(\frac{Q^{1/3}}{R} \right)^a \left(\frac{H}{R} \right)^\beta \quad (49)$$

The mentioned optimized formulae reflecting the elevation effect and the Eq. (44) undergo regression analysis. The obtained regression results are listed in Table 2.

Table 2 suggests that using the step (positive) formula to fit the monitoring data, the correlation coefficient is the largest, the degree of difference is the smallest, and the correction coefficient is the largest. This reveals that the formula fits the best. The correlation coefficient of the Sax (horizontal) formula fit is minimal. The degree of difference in the optimized formula 1 is the largest. The correction decision coefficient of the Saar (level) and optimized 1 formula fit is minimal. It shows that the Sax (horizontal) formula and the optimized 1 formula fit are inferior.

Table 2 Monitoring data regression results

Formula type	Formula	K	α	β	Cod(r^2)	Reduced chi-sqr	Adj.-Square
Sas (level)	$V = K(\frac{\sqrt{D}}{D})^\alpha$	379.6 8	1.57		0.8925	0.0587	0.8772
Saskatc hewan (space)	$V = K(\frac{\sqrt{D}}{\sqrt{D^2 + H^2}})^\alpha$	343.6 3	1.54		0.9012	0.0540	0.8871
Optimized 1	$V = K(\frac{\sqrt{D}}{D})^\alpha (\frac{\sqrt{D}}{H})^\beta$	169.6 6	1.20	0.28	0.9041	0.0611	0.8722
Optimized 2	$V = K(\frac{\sqrt{D}}{\sqrt{D^2 + H^2}})^\alpha (\frac{\sqrt{D}}{H})^\beta$	192.0 4	1.27	0.21	0.9068	0.0594	0.8757
Optimized 3	$V = K(\frac{\sqrt{D}}{\sqrt{D^2 + H^2}})^\alpha (\frac{H}{\sqrt{D^2 + H^2}})^\beta$	192.0 9	1.48	-0.21	0.9068	0.0594	0.8757
Step (positive)	$V = K(\frac{\sqrt{D}}{\sqrt{D^2 + H^2}})^\alpha (\frac{D}{\sqrt{D^2 + H^2}})^\beta$	216.7 4	1.37	7.41	0.9187	0.0518	0.8915

Notes: 1. Cod(r^2): characterizes the percentage of the variation according to the variable Y, as interpreted by the controlled independent variable X or representing the correlation coefficient;

2.Reduced Chi-Sqr: indicates the degree of direct difference between the observed value and the fitted value;

3. Adj. R-Square: The correction coefficient is one of the critical indicators to assess the quality of the model.

4.3 COMPARISON OF CALCULATION ACCURACY OF BLASTING VIBRATION SPEED

Using the regression results obtained in the previous section, the relative errors and the average errors between the monitoring data of Table 1 are compared, as well as the calculation results of the vibration velocity prediction formula of the reaction elevation effect. The comparison results are listed in Table 3 and Fig. 4.

Fig. 4 suggests that the Sa's (horizontal) formula has the largest prediction error, reaching 27.6%, followed by the Sa's (space) formula with an error of 23.5%; the step (positive) formula exhibits the smallest prediction error, only reaching 13.6%.

Table 3 Comparison of blasting vibration velocity prediction accuracy

Measuring point number	Measured value (cm/s)	Sa's Eq. (horizontal)		Sa's Eq. (space)		Optimized 1		Optimized 2		Optimized 3		Step (positive)	
		Forecast (cm/s)	Relative error	Forecast (cm/s)	Relative error	Forecast (cm/s)	Relative error	Forecast (cm/s)	Relative error	Forecast (cm/s)	Relative error	Forecast (cm/s)	Relative error
1	0.238	0.457	92.0%	0.415	74.4%	0.383	60.8%	0.368	54.5%	0.368	54.6%	0.301	26.5%
2	0.337	0.538	59.8%	0.509	51.1%	0.477	41.4%	0.467	38.6%	0.467	38.7%	0.446	32.4%
3	0.425	0.563	32.5%	0.530	24.7%	0.493	16.1%	0.483	13.6%	0.483	13.6%	0.452	6.4%
4	0.912	0.918	0.7%	0.920	0.8%	1.017	11.5%	0.989	8.4%	0.989	8.5%	1.044	14.5%
5	1.108	0.985	11.1%	0.984	11.2%	1.073	3.2%	1.045	5.6%	1.046	5.6%	1.102	0.6%
6	1.183	1.082	8.6%	1.075	9.1%	1.142	3.5%	1.117	5.6%	1.117	5.6%	1.175	0.7%
7	1.918	1.454	24.2%	1.426	25.7%	1.431	25.4%	1.409	26.5%	1.410	26.5%	1.452	24.3%
8	1.623	1.837	13.2%	1.808	11.4%	1.880	15.9%	1.840	13.4%	1.840	13.4%	1.865	14.9%
9	2.128	2.259	6.2%	2.203	3.5%	2.202	3.5%	2.165	1.7%	2.166	1.8%	2.167	1.8%
Average error		27.6%		23.5%		20.1%		18.7%		18.7%		13.6%	

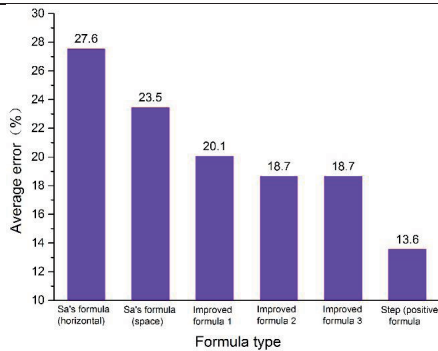


Figure 4 Comparison of vibration velocity prediction accuracies

5 CONCLUSION

Aiming at the height effect of bench blasting vibration, this paper uses theoretical research, field measurement and other methods to carry out research. Established a geometric model of the steps and analyzed the reflection of vibration waves on the free surface of the steps. Conducted on-site

monitoring and statistical analysis of blasting vibration. The main conclusions of the paper are as follows:

In this paper, we explain the mechanism of positive elevation effect and propose a formula for predicting the peak velocity of surface velocity, i.e. the step (positive) formula, in accordance with the reflection theory of elastic wave at the free interface.

This formula is employed to predict the peak vibration velocity of the surface blasting seismic wave and compare it with the measured value. It is found that this formula exhibits a significantly lower error of the prediction results than the commonly used Sa's formula at home and abroad and other optimized formulas. Accordingly, a more effective novel method is proposed for blasting vibration prediction.

The effectiveness and accuracy of the prediction method to predict the peak velocity of the surface elevation of the positive elevation difference in the step blasting project are verified, whereas the peak velocity of the ground in the negative elevation difference surface and the underground blasting project requires further prediction and verification.

REFERENCES

1. Wan Pengpeng et al. Research on the height effect of particle vibration velocity in step blasting. *Blasting*, 2015. 32(02): Page 29-32,63.
2. Jiang Nan et al., Rock slope blasting vibration velocity and elevation effect. *Journal of Central South University (Natural Science Edition)*, 2014. 45(01): 237-243.
3. Hu Guangqiu, Qu Shijie, Liang Xinmin, Research on the influence of elevation amplification effect on the attenuation of blasting vibration in open pits. *Huang Jin*, 2015. 36(07): pages 28-32.
4. Zhang, Y.J., G.Z. Wang and H.J. Zhang, Study on Numerical Simulation of Bench Blasting and its Elevation Amplification Effect. *Applied Mechanics & Materials*, 2012. 215-216: p. 1228-1231.
5. Peng, Y.X., et al., Study on the effect of elevation on the prediction of underwater drill and blasting vibration frequency. *Geosystem Engineering*, 2016. 19(4): p. 170-176.
6. Bhagade, N.V., V.M.S.R. Murthy and G. Budi, Measurement and control of seismic effects in large scale dragline bench blasts - An approach. *Measurement*, 2021. 168: p. 108390.
7. Tan Wenhui, etc., Analysis of the elevation effect of slope blasting vibration. *Chinese Journal of Geotechnical Engineering*, 2010. 32(4): 619-623.
8. Navarro Torres, V.F., et al., Assessing and controlling of bench blasting-induced vibrations to minimize impacts to a neighboring community. *Journal of Cleaner Production*, 2018. 187: p. 514-524.
9. Chen Ming et al., Study on the height amplification effect of blasting vibration velocity of rock slopes. *Chinese Journal of Rock Mechanics and Engineering*, 2011. 30(11): Page 2189-2195.
10. Havenith, H.B., et al., Initiation of earthquake-induced slope failure: influence of topographical and other site specific amplification effects. *Journal of Seismology*, 2003. 7(3): 397-412.
11. Nguyen, H., et al., Predicting blast-induced peak particle velocity using BGAMs, ANN and SVM: a case study at the Nui Beo open-pit coal mine in Vietnam. *Environmental Earth Sciences*, 2019. 78(15).
12. Mohammadi Azizabadi, H.R., H. Mansouri and O. Fouché, Coupling of two methods, waveform superposition and numerical, to model blast vibration effect on slope stability in jointed rock masses. *Computers and Geotechnics*, 2014. 61: 42-49.
13. Hu Xuelong et al. Attenuation law of blasting seismic waves based on equivalent paths. *Explosion and Shock*, 2017. 37(06): 966-975.
14. Guo Xuebin, Xiao Zhengxue, Zhang Zhicheng, Slope effect of blasting vibration. *Chinese Journal of Rock Mechanics and Engineering*, 2001(01): 83-86.

15. Zhou Tongling, Yang Xiufu, Weng Jiajie, Experimental Study on the Elevation Effect of Blasting Vibration. *Well Construction Technology*, 1997(S1): 32-36.
16. Feng Zhiren, Liu Hongshuai, Yu Long, Study on the surface amplification effect of bedding rock slopes with weak interlayers under earthquake action. *Journal of Disaster Prevention and Mitigation Engineering*, 2014. 34(01): 96-100.
17. Yang, D., et al., Experiment and Analysis of Wedge Cutting Angle on Cutting Effect. *Advances in Civil Engineering*, 2020. 2020, Article ID 5126790
18. An, H.M., et al., Hybrid finite-discrete element modelling of dynamic fracture and resultant fragment casting and muck-piling by rock blast. *Computers and Geotechnics*, 2017. 81: p. 322-345.
19. An, H., H. Liu and H. Han, Hybrid Finite-Discrete Element Modelling of Excavation Damaged Zone Formation Process Induced by Blasts in a Deep Tunnel. *Advances in Civil Engineering*, 2020. 2020, Article ID 7153958
20. Liu Xiwu, *Fundamentals of Elastic Wave Field Theory*. 2008, Qingdao: Ocean University of China Press.
21. R. E. Sheriff, L.P.G., *Exploration Seismology*. 1983: CAMBRIDGE UNIVERSITY PRESS.
22. Lu Jimeng, *Principles of Seismic Exploration (Volume 2)*. 1993, Dongying, Shandong: China University of Petroleum Press.
23. Wang Lili, *Fundamentals of Stress Waves (2nd Edition)*. 2005, Beijing: National Defense Industry Press.
24. Xiao Zhengxue, Zhang Zhicheng, Li Chaoding, Blasting seismic wave dynamics and seismic effects. 2004, Chengdu: University of Electronic Science and Technology Press.
25. Guillaume, G., et al., Time-domain impedance formulation for transmission line matrix modelling of outdoor sound propagation. *Journal of Sound & Vibration*, 2011. 330(26): p. 6467-6481.
26. Meng Jifu, Hui Hongbin, *Blasting Testing Technology*. 1992, Beijing: Metallurgical Industry Press.
27. National Development and Reform Commission of the People's Republic of China, *Technical Code for Construction of Rock Foundation Excavation Engineering of Hydraulic Structure, SL-941994*, Water Resources and Hydropower Press: Beijing.
28. Zhu Chuazhong, Liu Honggen, Mei Jinyu, Selection of the formula for the propagation law of seismic wave parameters along the slope. *Blasting*, 1988(02): 30-31.
29. Tang Hai, Li Haibo, Research on the blasting vibration formula reflecting the elevation amplification effect. *Rock and Soil Mechanics*, 2011. 32(03): 820-824.

LIST OF FIGURES AND TABLES:

Figure 1 P wave incidence

Figure 2 Step model and flat model

Figure 3. Vibration velocity of measuring point

Figure 4 Comparison of vibration velocity prediction accuracies

Table 1 Measurement point blasting vibration monitoring data

Table 2 Monitoring data regression results

Table 3 Comparison of blasting vibration velocity prediction accuracy

Received: 16.10.2020, Revised: 30.11.2020